

# EXTREME CIRCUMGALACTIC H I AND C III ABSORPTION AROUND THE MOST MASSIVE, QUENCHED GALAXIES

MARIJANA SMILAGIĆ,<sup>1</sup> JASON XAVIER PROCHASKA,<sup>1</sup> JOSEPH BURCHETT,<sup>1</sup> GUANGTUN ZHU,<sup>2</sup> AND BRICE MÉNARD<sup>2</sup>

<sup>1</sup>*University of California, 1156 High Street, Santa Cruz, CA 95064, USA*

<sup>2</sup>*Johns Hopkins University, 3400 N. Charles Street, Baltimore, MD 21218, USA*

Submitted to ApJ

## ABSTRACT

Luminous red galaxies (LRGs) are the most massive galaxies at  $z \sim 0.5$  and, by selection, have negligible star formation. These objects have halo masses between those of  $L_*$  galaxies, whose circumgalactic media (CGM) are observed to have large masses of cold gas, and clusters of galaxies, which primarily contain hot gas. Here we report detections of strong and extended metal (C III 977) and H I lines in the CGM of two LRGs. The C III lines have equivalent widths of  $\sim 1.8 \text{ \AA}$  and  $\sim 1.2 \text{ \AA}$ , and velocity spreads of  $\sim 796 \text{ km s}^{-1}$  and  $\sim 1245 \text{ km s}^{-1}$ , exceeding all such measurements from local  $\sim L_*$  galaxies (maximal C III equivalent widths  $\sim 1 \text{ \AA}$ ). The data demonstrate that a subset of halos hosting very massive, quenched galaxies contain significant complexes of cold gas. Possible scenarios to explain our observations include that the LRGs CGM originate from past activity (e.g., star formation or active galactic nuclei driven outflows) or from the CGM of galaxies in overlapping subhalos. We favor the latter scenario, in which the properties of the CGM are more tightly linked to the underlying dark matter halo than properties of the targeted galaxies (e.g., star formation).

*Keywords:* galaxies: formation — galaxies: halos — intergalactic medium — quasars: absorption lines

arXiv:1809.09777v1 [astro-ph.GA] 26 Sep 2018

## 1. INTRODUCTION

A series of absorption-line surveys piercing the halos of individual galaxies have established the near-ubiquitous presence of a large reservoir of cool and enriched gas in the circumgalactic environment. This cool circumgalactic medium (CGM) is manifest in galaxies with a wide range of luminosity and across most of cosmic time (e.g., Tumlinson et al. 2017; Chen 2017). In the ‘normal’ population of field galaxies, one now recognizes the cool CGM as a fundamental baryonic component of galaxies and, therefore, a main cog in the machinery of galaxy formation.

From this ensemble of observational CGM studies, several key trends and puzzles emerge. Of particular interest to this work is the apparent correlation between the absorption strength of the cool CGM and galaxy mass (Chen et al. 2010; Prochaska et al. 2011, 2014). Most recently, Bordoloi et al. (2017) has emphasized a strong correlation between the Ly $\alpha$  equivalent width (EW) and the galaxy stellar mass in present-day,  $L \lesssim L^*$  galaxies. These authors interpret the increase in EW with stellar mass as a fundamental relation between the CGM dynamics and the underlying dark matter halo mass. Another, more puzzling, result that has materialized is the preponderance of this cool CGM even around quiescent galaxies (Thom et al. 2012; Zhu et al. 2014; Huang et al. 2016; Zahedy et al. 2016; Tumlinson et al. 2017; Chen 2017), but see also Lan et al. (2014). Despite an interstellar medium in many cases nearly devoid of cool gas and minimal active star-formation (e.g., Young et al. 2014), these galaxies exhibit CGM with HI and low-ionization metal content comparable to the star-forming population. Extrapolating these two results to higher mass halos, where red and dead galaxies proliferate, one might conclude that galaxy clusters may harbor the largest mass of cool halo gas in the universe.

This assertion, however, runs contrary to observations of the hot intracluster medium in galaxy clusters (Mitchell et al. 1976) and theoretical work which predicts a predominantly virialized gas (Voit 2005; Dekel & Birnboim 2006; Kravtsov & Borgani 2012). And, indeed, the few studies that have examined the cool CGM of galaxy clusters support a suppressed incidence of such gas both within the halo and within the halos of the cluster members (Burchett et al. 2018; Yoon & Putman 2017), but see also Lopez et al. (2008). These results, while still sparse, suggest a rapid decline in the cool CGM in the most massive halos.

Another opportunity to extend CGM studies into the high halo-mass regime is afforded by the set of over 1 million luminous red galaxies (LRGs) discovered in the Sloan Digital Sky Survey (Dawson et al. 2013). These

galaxies have inferred halo masses  $\approx 10^{13.5} M_\odot$  (White et al. 2011) and, by selection, have negligible on-going star formation. Focusing on the Mg II doublet (the best cool CGM diagnostic available at optical wavelengths for intermediate redshifts), CGM surveys of LRGs have demonstrated a lower incidence of such gas than around  $L^*$  galaxies, with covering fraction of  $\sim 5\%$  (e.g., Huang et al. 2016). Nevertheless, the full statistical power of the BOSS experiment has revealed a strong excess in the cross-correlation between Mg II and the LRG within the virial radius (Zhu et al. 2014, and references therein) Furthermore, the relation of estimated mean EW with impact parameter approaches that of  $L^*$  galaxies (Prochaska et al. 2014, fig. 10).

Inspired by the Zhu et al. (2014) survey, we pursued far-UV observations for a modest sample (15) of QSO sightlines probing the LRG-CGM. Our data access the strong H I Lyman series and metal-line transitions that trace intermediate (e.g. C III) and highly ionized gas (O VI) at the LRG redshifts, which ground-based surveys did not. In this Letter, we report on the surprising detection of two LRGs whose cool CGM absorption exceeds that of all previous measurements of  $L \sim L^*$  galaxies. This manuscript is organized as follows: In Section 2, we briefly describe the data and spectral line measurements. Section 3 puts these two LRGs in the broader context of CGM observations and discusses the origin of our extreme CGM cases.

## 2. DATA, SAMPLE AND MEASUREMENTS

The two LRG-QSO pairs analyzed here are taken from a larger survey studying the CGM of LRGs, which we describe here briefly. The SDSS-III/Baryon Oscillation Spectroscopic Survey (BOSS; Dawson et al. 2013) contains over  $10^6$  spectra of LRGs at redshifts  $z \sim 0.5$ . We matched LRGs from the BOSS survey and QSOs from the SDSS DR12 survey (Pâris et al. 2017), such that the projected distance between the QSO and the LRG (impact parameter) is less than 400 kpc, and the LRG has a redshift  $z_{\text{LRG}} > 0.4$ . From this sample we selected 15 pairs where the quasars have bright GALEX magnitudes and where approximately half were previously known to exhibit MgII absorption in the LRG-CGM (Zhu et al. 2014). A complete survey description is forthcoming by Smailagić et al. (2018, in preparation).

Images from the Sloan Digital Sky Survey (SDSS) of LRG\_1059+4039 and LRG\_1440-0156 are shown in Figure 1. Both LRGs are located at  $z \sim 0.5$  and have impact parameters of  $\sim 30$  kpc and  $\sim 350$  kpc, typical of the full sample. The bottom panel in Figure 1 shows

the impact parameter (scaled to the virial radius<sup>1</sup>) versus the stellar mass  $M_*$  for our full sample of 15 LRGs; galaxies from the COS-Halos survey (Werk et al. 2012) are also plotted for reference.

We obtained HST COS spectra of the 15 QSOs in Cycle 23 (GO-14171 ; PI Guangtun Zhu). We used the G140L grating with resolving power  $R \sim 2000 - 3000$  for the wavelengths of interest (spectral resolution  $\sim 150 \text{ km s}^{-1}$ ). Wavelength coverage for the segment A is  $\sim 1300 - 2000 \text{ \AA}$ , and signal-to-noise ratio per pixel is  $\sim 4 - 6$ . Data were reduced using the CALCOS v2.21 software package and our own custom Python codes<sup>2</sup>. Our modifications to the CALCOS software follow those described by Worseck et al. (2016), and include a modified estimate of the dark current and modified co-addition of sub-exposures. In the reduced spectra, the quasar continuum was estimated by generating a cubic spline ‘anchor’ points set by eye using the `lt_continuumfit` GUI of the LINETOOLS package<sup>3</sup>. Absorption lines were identified with the `igmguesses` tool from the PYIGM package<sup>4</sup>. EWs were calculated from box-car integration across the absorption complex. Line detections are considered reliable if their EWs exceed three times their estimated uncertainties.

Regarding line-identification, which is non-trivial for sightlines to  $z \sim 1$  quasars, we first identified strong lines in the Milky Way and those associated with the QSO. We then searched for lines near the LRG redshift, beginning with the H I Lyman series and proceeding to metal-line transitions. We also searched for unrelated, strong absorption systems along the sightline that could present interloping absorption with the LRG-CGM lines. A subset of the transitions identified with the LRG-CGM is shown in Figures 2 and 3. It is evident that these galaxies exhibit very strong low, intermediate, and even high-ion absorption. One also notes that the strongest low and intermediate-ion absorption is coincident with the largest optical depth of Mg II from the SDSS QSO spectra.

To further confirm the line identifications, Figures 2 and 3 also compare scaled apparent column densities of C III 977 and H I transitions. For example, from Figure 3 we see that the scaled apparent column density

profiles for C III 977 and H I 1025 are consistent in the velocity range from  $\sim -300$  to  $400 \text{ km s}^{-1}$ . At velocities  $> 400 \text{ km s}^{-1}$ , the C III line is possibly blended, or the physical conditions of the gas may differ, changing the C III/H I ratio as well. This close alignment between the absorption from these two species over such a large velocity range corroborates the identification of this system while revealing an extraordinary complex of metal-enriched gas in the CGM of the LRG. We find similar results for LRG\_1059+4039 and for the other H I transitions.

Next, we measure the velocity spread  $\Delta v_{90}$  for C III 977, which is defined as the velocity interval containing 90% of the total optical depth (Prochaska & Wolfe 1997). Pixels where flux is below noise level were replaced with the noise. The two LRGs have  $\Delta v_{90} \sim 945$  and  $\sim 760 \text{ km s}^{-1}$ , respectively. These values will decrease by  $\sim 100 \text{ km s}^{-1}$  if consider the COS spectrograph resolution. We also caution that the C III 977 lines are saturated. The Ly $\alpha$  lines are also saturated, but we obtain  $\Delta v_{90, \text{Ly}\alpha} = 1497$  and  $640 \text{ km s}^{-1}$  if we measure them in the same manner.

### 3. RESULTS AND DISCUSSION

The spectra shown in Figures 2 and 3 demonstrate the presence of extremely strong, cool CGM absorption-profiles surrounding LRG\_1059+4039 and LRG\_1440-0156. To provide context, we compare the measured C III 977 EWs against the data for low- $z$   $L^*$  galaxies from the COS-Halos survey (Figure 4; Werk et al. 2013). The C III EWs of the two LRG CGM ( $\sim 1.8 \text{ \AA}$  and  $\sim 1.2 \text{ \AA}$ ) clearly exceed the entire  $L^*$  galaxy distribution. In fact, the LRG\_1059+4039 C III absorption is nearly twice as strong as the  $L^*$  CGM maximum. To date, the only other population of galaxies known to exhibit such strong and extended absorption lines are QSO host galaxies at  $z \sim 2$  (Prochaska et al. 2013; Lau et al. 2016) and ultra-strong Mg II absorbers (e.g., Nestor et al. 2011). We note that a few other individual examples of large low-ion EWs associated with the CGM of luminous red or massive elliptical galaxies (Gauthier 2013; Zahedy et al. 2016) have been reported. However, none of these studies found metal UV transitions exceeding those of  $L_*$  galaxies. Figure 4 also shows that our two LRGs and some of the  $L_*$  galaxies exceed other known LRGs CGM with available C III measurements (recently studied by Chen et al. 2018). We note that certain  $L^*$  galaxies are associated with ultra-strong Mg II absorbers (e.g., Nestor et al. 2011); however, these associations are rare and are possibly (post-)starbursts. Nevertheless, C III measurements are not available for these strong absorbers. Using the combined sample of

<sup>1</sup> We estimate halo masses from stellar masses and Moster et al. (2010) relation between stellar and dark matter halo mass. Stellar masses are used from the Wisconsin group, wisconsin\_pca\_m11-DR12-boss.fits.gz [http://www.sdss.org/dr14/spectro/galaxy\\_wisconsin/](http://www.sdss.org/dr14/spectro/galaxy_wisconsin/) ) Virial radius is calculated as for COS-Halos in Tumlinson et al. (2013).

<sup>2</sup> [https://github.com/PYPIT/COS\\_REDUX](https://github.com/PYPIT/COS_REDUX)

<sup>3</sup> <https://github.com/linetools/linetools>

<sup>4</sup> <https://github.com/pyigm/pyigm>

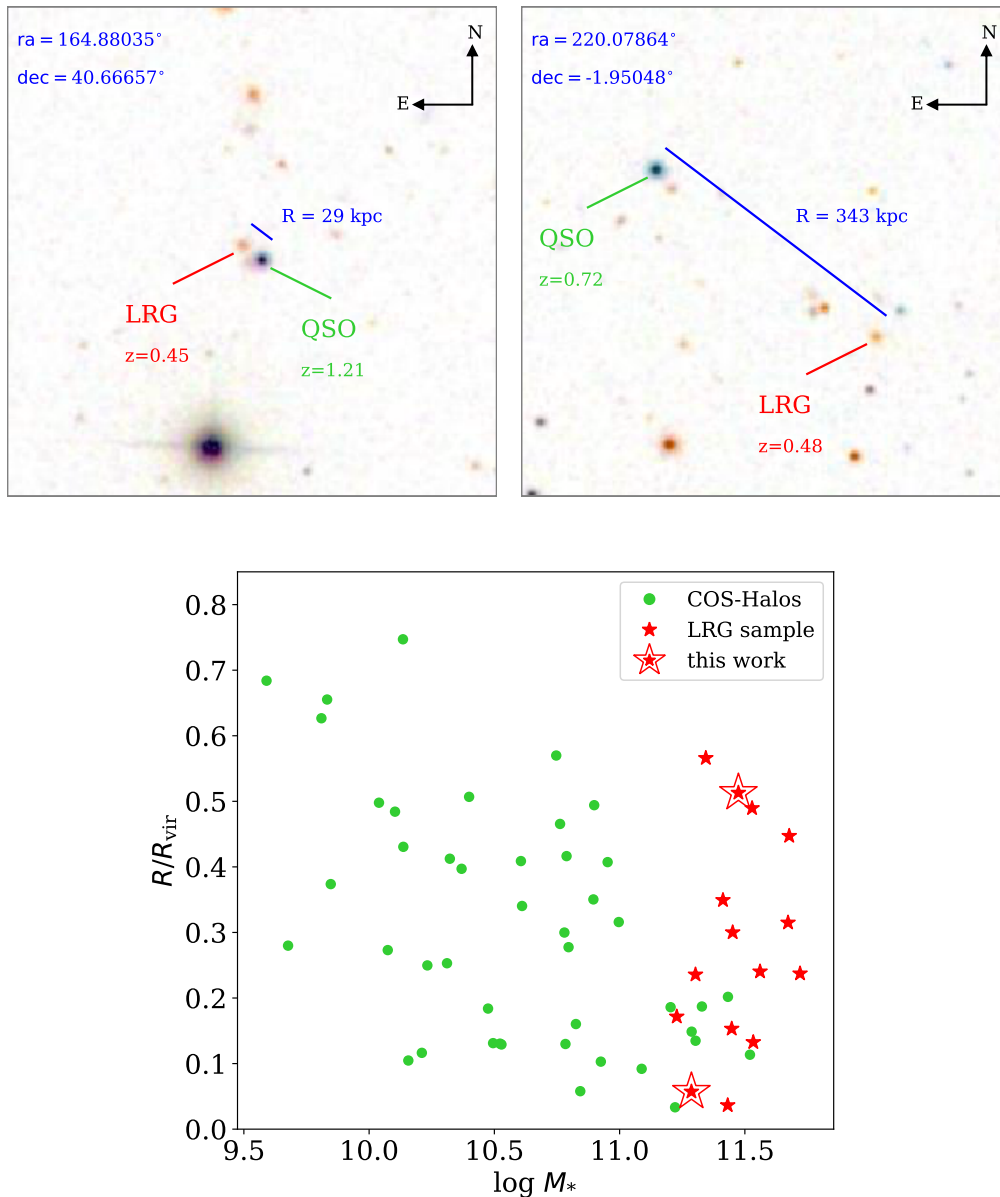


**Figure 1.** Top: SDSS images of the two LRGs. The LRG coordinates are given in the upper left corner. Bottom: Impact parameter  $R$  scaled to the virial radius  $R_{\text{vir}}$  versus stellar mass  $M_*$  for LRGs and COS-Halos.

COS-Halos (Werk et al. 2013) and our sample of LRGs, a Spearman correlation test shows a  $\sim 5$ -sigma correlation between  $\text{EW}(\text{C III})$  and  $\text{EW}(\text{Mg II})$ , see Figure 5. This indicates that C III and Mg II might track one another. However, the scatter in this relation is  $\sim 1 \text{ \AA}$ , and if we fit a linear relation between  $\text{EW}(\text{C III})$  and  $\text{EW}(\text{Mg II})$ , then for 3 of 7 LRGs, the difference between the measured and predicted  $\text{EW}(\text{C III})$  will be greater than  $0.4 \text{ \AA}$  (for all COS-Halos systems, the differences

are  $\lesssim 0.4 \text{ \AA}$ ). For example, one of the large-EW(C III) LRGs featured in this work shows an  $\text{EW}(\text{Mg II})$  that lies  $\sim 1 \text{ \AA}$  below this would-be relation and in fact has a smaller  $\text{EW}(\text{Mg II})$  than several of the  $\text{EW}(\text{C III}) < 1 \text{ \AA}$  COS-Halos and LRG systems. In addition, the same correlation for absorbers with  $\text{EW}(\text{C III}) > 0.5 \text{ \AA}$  (LRGs from our full sample, COS-Halos, Chen et al. (2018) galaxies) is significant to only  $1.1 \sigma$ . Given this and the large scatter in a such a correlation, we contend

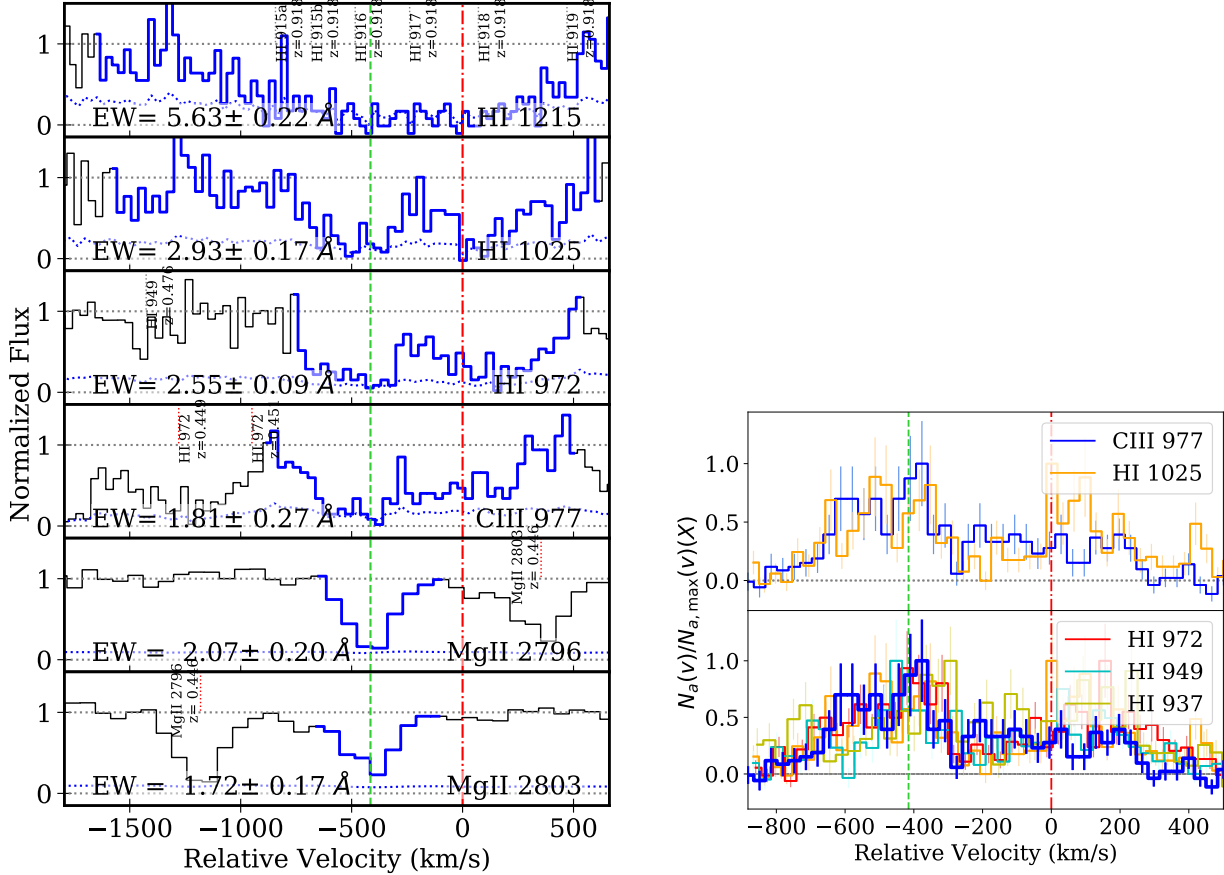


**Figure 2.** Left: Line profiles for LRG\_1059+4039: H I 1215, H I 1025, H I 972, C III 977, Mg II 2796, and Mg II 2803. The analyzed velocity ranges are marked in blue. Interloping transitions in each panel are labeled in red if they originate from the same LRG CGM system, otherwise in gray. Rest frame equivalent widths are shown in the lower left corner. The dotted blue line represents the flux uncertainty. Right: Apparent column densities of the C III and H I transitions associated with LRG\_1059+4039, scaled such that the maximum of each is unity. Velocities at the redshifts of the LRG and Mg II absorption are marked with red dot-dashed and green dashed vertical line, respectively.

that Mg II and C III offer independent information on the CGM of LRGs. Certainly, the presence of Mg II absorption does not ensure such strong and widely extended C III as we report here (cf. the Mg II and C III profiles in Figs. 2 and 3)

Similar to the EW measurements, the C III  $\Delta v_{90}$  are also much larger for these LRGs. COS-Halos have  $\Delta v_{90}$  values up to  $\sim 407 \text{ km s}^{-1}$  and average line widths of  $\sim 196 \text{ km s}^{-1}$  (when smoothed to the same resolution as our QSO-LRGs spectra), which are two to a few times smaller than the LRGs presented here. As with C III, the two LRGs also exhibit very strong H I absorption (with H I 1215  $\sim 5.6 \text{ \AA}$  and  $\sim 1.7 \text{ \AA}$ , and column densities from the Lyman-limit flux decrement  $\sim 10^{17.68} \text{ cm}^{-2}$  and  $\sim 10^{16.99} \text{ cm}^{-2}$ ), and the LRG\_1059+4039 H I EW exceeds that of all COS-Halos systems. These two LRGs represent extrema of the CGM.

We turn now to discuss the origin of this extreme CGM. Previous studies examining systems with large EWs and/or large velocity widths have frequently invoked non-gravitational motions associated with feedback processes that have ejected significant mass from the central galaxy. This includes winds driven from bursts of star-formation (e.g., Rubin et al. 2014; Heckman et al. 2017) and outflows driven by AGN activity (e.g., Tripp et al. 2011). In our experiment, the targeted galaxies are ‘red and dead’ with negligible current star-formation (SF) and no signature of SF activity over at least the past Gyr. Therefore, we rule out feedback from recent star-formation from LRGs as a viable origin for the observed CGM.

We have also searched for any signatures of AGN activity from our targeted LRGs or any neighboring galaxies. Within 2 arcmin of each LRG, there are no sources detected in the Faint Images of the Radio Sky

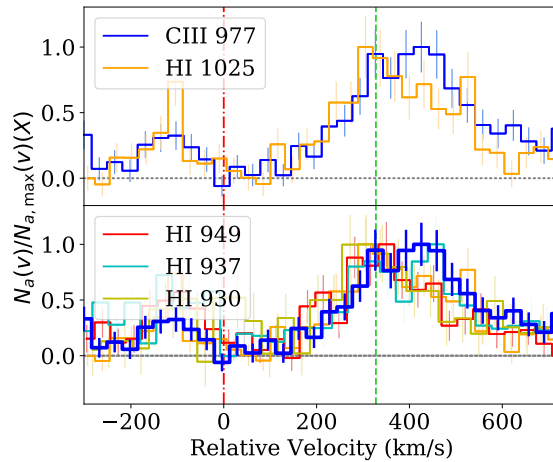
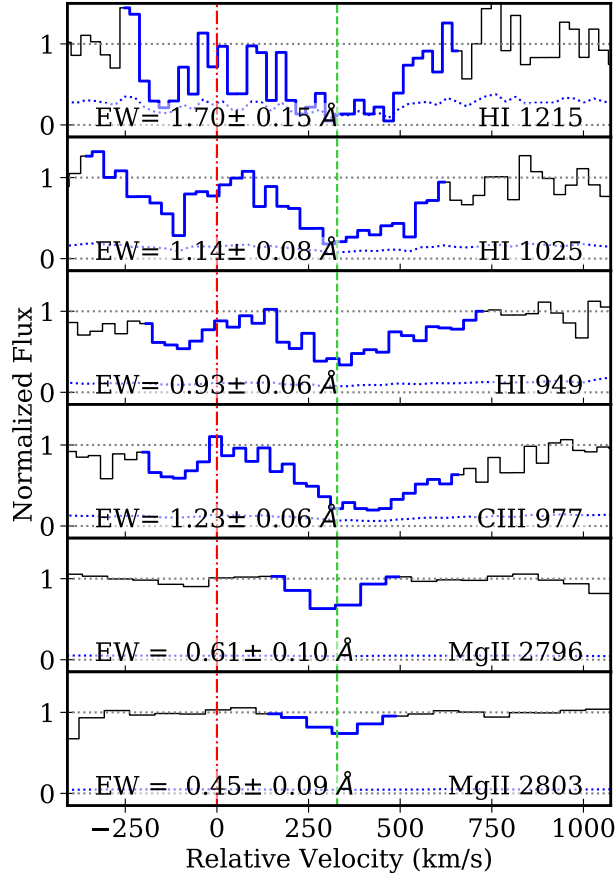


**Figure 3.** Same as Figure 2, but for LRG\_1440-0156.

at Twenty-Centimeters (FIRST) survey (Becker et al. 1995). From the Wide-field Infrared Survey Explorer (WISE; Wright et al. 2010), there are several sources in the LRG fields but all of these have color  $W1 - W2 \ll 0.8$  (most have  $W1 - W2 \sim 0.1$ ), indicating that the emission is of stellar origin (Stern et al. 2012). Together the FIRST non-detections and the WISE colors indicate the absence of any active AGN for galaxies near the quasar sightlines.

In addition to outflows from forming stars and AGN, gas may be pulled from galaxies through gravitational interactions (i.e., tidal stripping). However, the observed velocity range in tidal streams of local interacting galaxies is typically  $\sim 100 \text{ km s}^{-1}$  (Hibbard & van Gorkom 1996) with a few cases exceeding  $100 \text{ km s}^{-1}$  (Weilbacher et al. 2003). Given the observed  $\sim 1000 \text{ km s}^{-1}$  velocity spread in the LRG-CGM, we consider tidal interactions to be a sub-dominant contribution.

Inflows of cold gas from the intergalactic medium are also disfavored because they are predicted to have low metallicity and correspondingly much lower EWs than what we have observed (Fumagalli et al. 2011). Furthermore, the predicted kinematics for this infalling gas im-

ply modest velocities ( $\approx 100 \text{ km s}^{-1}$ , Nelson et al. 2016) and these cold flows are not expected to frequent massive halos (Dekel & Birnboim 2006; Kereš et al. 2009).

Absent an active source to produce the extreme CGM signatures of our target LRGs, we must consider alternate origins. One possibility is that this gas is a relic of previous activity within the LRG (the most luminous galaxy in the halo). For example, cold CGM clouds could have formed at higher redshifts, when LRGs were intensely forming stars or contained an AGN. This could provide an intragroup medium with significant cool gas absorption (Gauthier 2013). Indeed, the CGM of QSO host galaxies contains large amounts of cold gas and has comparably extended and strong H I and metal lines (e.g., Prochaska et al. 2013; Lau et al. 2016). Furthermore, the dark matter halos hosting  $z \sim 2$  quasars have estimated masses  $\sim 10^{12.5} M_{\odot}$  (White et al. 2012) and one predicts that a non-negligible fraction will evolve into the halos hosting LRGs. The obvious challenge to this scenario, however, is that the cool gas must survive for several Gyr while not accreting onto a galaxy or being heated as the halo virializes.

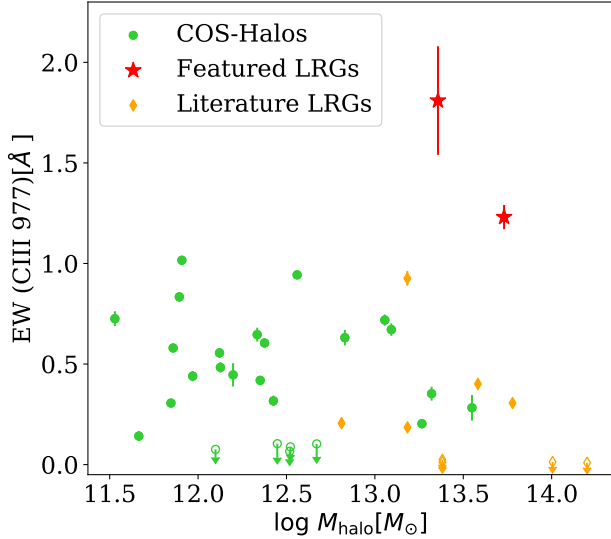


**Figure 4.** Rest frame EW of the C III 977 Å line versus dark matter halo mass for our two LRGs (red stars) compared with COS-Halos (green circles) and literature LRGs (orange diamonds; Chen et al. 2018)<sup>a</sup> EWs for the two LRGs exceed those of all COS-Halos galaxies, and the corresponding EW for LRG\_1059+4039 is nearly twice the COS-Halos maximum.

<sup>a</sup> We found that in Chen et al. (2018) LRGs are defined differently than as originally defined in BOSS survey (see e.g. LRGs coordinates list in [http://www.sdss.org/dri14/spectro/galaxy\\_wisconsin/](http://www.sdss.org/dri14/spectro/galaxy_wisconsin/)), and we display only their LRGs that were initially defined as such.

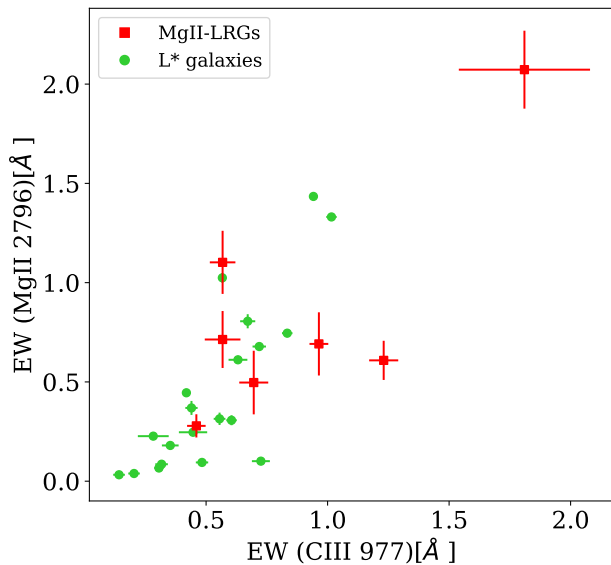


**Figure 5.** Equivalent width in Mg II 2796 versus equivalent width in C III 977 for COS-Halos (green circles) and LRGs from our full sample (red squares).

On the point of cloud survival, idealized hydrodynamic studies of cool gas clouds moving through a hot and more diffuse halo indicate that the largest sized clumps ( $r > 250$  pc) may survive for hundreds of Myr (Armillotta et al. 2017). Even a population of such very large clouds, however, are predicted to shed the majority of their mass after several Gyr (extrapolating from the published mass loss rates). Over time, less massive clouds would be destroyed, possibly explaining why the covering fraction of LRGs is low but certain sightlines have large amounts of cold gas detected.

The scenario we favor is that our LRG-CGM absorbers originate from gas in overlapping projected subhalos throughout the larger dark matter halo. In contrast to  $L^*$  galaxies, where low-mass satellites are unlikely to contribute significantly to the observed cool CGM (Tumlinson et al. 2013), the halos hosting LRGs may contain many luminous ( $L \sim L^*$ ) satellite galaxies. To explore this hypothesis, we have searched for galaxies in the SDSS imaging catalog whose photometric redshifts are consistent with the LRG redshift  $z_{\text{LRG}}$  (i.e.,  $|z_{\text{LRG}} - z_{\text{phot}}| < \sigma(z_{\text{phot}})$ ), hereafter, neighboring galaxies (NGs). Placing these sources at the LRG redshifts, we identify 3 galaxies within  $R < 100$  kpc of each of the QSO\_1059+4039 and QSO\_1440-0156 sightlines and several additional galaxies with  $R = 100 - 200$  kpc. All NGs around LRG\_1059+4039 have red colors with  $u-r > 0.9$ , except one (4 red, 1 blue), while only one of the 4 galaxies around LRG\_1440-0156 has a red color. Not including LRGs, and assuming that at  $z \sim 0.5$  absolute magnitude  $M_g \sim -20.4$  corresponds to  $L_*$  galaxies (Skibba et al. 2013, and references therein), the  $g$ -band luminosities of the nearby galaxies are  $\sim 0.6 - 1.5L_*$ .

We offer a few additional comments on several specific galaxies. One of the 3 galaxies around QSO\_1059+4039 is located very close to the QSO sightline ( $\approx 2''$ ), and is not cataloged by the SDSS survey but is detected in the Panoramic Survey Telescope and Rapid Response System (Pan-STARRS) images. In addition, another LRG with somewhat higher stellar mass lies  $\sim 200$  kpc away from the QSO\_1059+4039 sightline and is offset by only  $\approx +200$  km  $s^{-1}$  from the target LRG. Lastly, we comment that the redMaPPer survey (Rykoff et al. 2014) identifies a cluster of galaxies near LRG\_1059+4039 (at distance 1.68' and with a consistent redshift) and no clusters within 5' of LRG\_1440-0156. In addition, these two LRGs occupy 2/3 of the most densely populated environments in our full sample (Smailagić et al. 2018, in preparation).

We now explore whether the overlapping CGM of  $\sim 5$  luminous galaxies within 200 kpc of the sightline is sufficient to reproduce the observed EW and  $\Delta v$  values. The

estimated line-of-sight velocity dispersion for galaxies in a dark matter halo of  $10^{13.5} M_{\odot}$  is  $\sigma_{1D} \approx 286 \text{ km s}^{-1}$ . If we randomly sample a Gaussian distribution with  $\sigma_{1D}$ , the average velocity spread for 5 galaxies is  $\sim 665 \text{ km s}^{-1}$ , and  $2 \sigma$  range is  $\sim 172 - 1158 \text{ km s}^{-1}$ . If each of these galaxies exhibits a CGM comparable to present-day  $L^*$  galaxies ( $\approx 124 \text{ km s}^{-1}$  for COS-Halos), we recover a velocity width that is comparable to the observed velocity spreads.

Next, consider the observed EWs. For every NG within 200 kpc of the QSO sightline, we estimate the stellar mass using rest-frame absolute magnitudes from SDSS and the correlation between stellar mass and absolute red magnitude from Liang & Chen (2014):  $\log M_* = 0.14 - 0.49 M_{sdss,r}$ . Following Bordoloi et al. (2017), we estimate the Ly $\alpha$  EWs from these NGs as  $\log W_{HI1215} = 0.34 - 0.0026R + 0.286 \log M_*$ , where  $R$  is the impact parameter between galaxies and QSO. For the targeted LRGs only, we obtain EW  $3.1 \text{ \AA}$  and  $0.5 \text{ \AA}$ , which are smaller than observed. If we strictly add the Ly $\alpha$  EWs from the galaxies within 200 kpc, we obtain  $6.9 \text{ \AA}$  and  $5.1 \text{ \AA}$ . When we take into account that the covering fraction for red galaxies in COS-Halos is  $\sim 75\%$  (Tumlinson et al. 2013), the calculated EWs are  $\sim 7.3$  and  $3.8 \text{ \AA}$ , larger than the observed EWs. However,

the total predicted EWs would decrease if we allow for overlapping absorption if the sum is a saturated line. Furthermore, one may expect the galaxies in dense environments to have smaller EWs (see, e.g., Burchett et al. 2018), or several of the galaxies may be at unrelated redshifts.

The overlapping subhalos CGM scenario is consistent with the multiple line components observed in our LRGs' CGM and their large velocity spread. For example, the cold CGM could originate from outflows from blue NGs, or survive (e.g., Armillotta et al. 2017) or reform (e.g., Thompson et al. 2016) from earlier times.

In turn, our results support scenarios where the properties of the CGM are more tightly linked to the underlying dark matter halo than properties of the targeted galaxies (e.g., star-formation), (e.g., Zhu et al. 2014). This scenario could also be tested by obtaining spectra of the putative satellite galaxies of these two LRGs to confirm their membership and assess their properties. The results presented here reveal that when cool CGM are present in massive halos, the associated absorption may greatly exceed that in lower mass systems.

## REFERENCES

- Armillotta, L., Fraternali, F., Werk, J. K., Prochaska, J. X., & Marinacci, F. 2017, MNRAS, 470, 114
- Becker, R. H., White, R. L., & Helfand, D. J. 1995, ApJ, 450, 559
- Blanton, M. R., Hogg, D. W., Bahcall, N. A., et al. 2003, ApJ, 592, 819
- Bordoloi, R., Prochaska, J. X., Tumlinson, J., et al. 2017, arXiv:1712.02348
- Burchett, J. N., Tripp, T. M., Wang, Q. D., et al. 2018, MNRAS, 475, 2067
- Chen, H.-W., Wild, V., Tinker, J. L., et al. 2010, ApJL, 724, L176
- Chen, H.-W. 2017, Gas Accretion onto Galaxies, 430, 167
- Chen, H.-W., Zahedy, F. S., Johnson, S. D., et al. 2018, MNRAS, 479, 2547
- Dawson, K. S., Schlegel, D. J., Ahn, C. P., et al. 2013, AJ, 145, 10
- Dekel, A., & Birnboim, Y. 2006, MNRAS, 368, 2
- Fumagalli, M., Prochaska, J. X., Kasen, D., et al. 2011, MNRAS, 418, 1796
- Gauthier, J.-R. 2013, MNRAS, 432, 1444
- Heckman, T., Borthakur, S., Wild, V., Schiminovich, D., & Bordoloi, R. 2017, ApJ, 846, 151
- Hibbard, J. E., & van Gorkom, J. H. 1996, AJ, 111, 655
- Huang, Y.-H., Chen, H.-W., Johnson, S. D., & Weiner, B. J. 2016, MNRAS, 455, 1713
- Kereš, D., Katz, N., Fardal, M., Davé, R., & Weinberg, D. H. 2009, MNRAS, 395, 160
- Kravtsov, A. V., & Borgani, S. 2012, ARA&A, 50, 353
- Lan, T.-W., Ménard, B., & Zhu, G. 2014, ApJ, 795, 31
- Lau, M. W., Prochaska, J. X., & Hennawi, J. F. 2016, ApJS, 226, 25
- Liang, C. J., & Chen, H.-W. 2014, MNRAS, 445, 2061
- Lopez, S., Barrientos, L. F., Lira, P., et al. 2008, ApJ, 679, 1144
- Mitchell, R. J., Culhane, J. L., Davison, P. J. N., & Ives, J. C. 1976, MNRAS, 175, 29P
- Moster, B. P., Somerville, R. S., Maulbetsch, C., et al. 2010, ApJ, 710, 903
- Nelson, D., Genel, S., Pillepich, A., et al. 2016, MNRAS, 460, 2881
- Nestor, D. B., Johnson, B. D., Wild, V., et al. 2011, MNRAS, 412, 1559
- Pâris, I., Petitjean, P., Ross, N. P., et al. 2017, A&A, 597, A79
- Prochaska, J. X., & Wolfe, A. M. 1997, ApJ, 487, 73



- Prochaska, J. X., Weiner, B., Chen, H.-W., Mulchaey, J., & Cooksey, K. 2011, *ApJ*, 740, 91
- Prochaska, J. X., Hennawi, J. F., & Simcoe, R. A. 2013, *ApJL*, 762, L19
- Prochaska, J. X., Lau, M. W., & Hennawi, J. F. 2014, *ApJ*, 796, 140
- Rubin, K. H. R., Prochaska, J. X., Koo, D. C., et al. 2014, *ApJ*, 794, 156
- Rykoff, E. S., Rozo, E., Busha, M. T., et al. 2014, *ApJ*, 785, 104
- Skibba, R. A., Sheth, R. K., Croton, D. J., et al. 2013, *MNRAS*, 429, 458
- Stern, D., Assef, R. J., Benford, D. J., et al. 2012, *ApJ*, 753, 30
- Thom, C., Tumlinson, J., Werk, J. K., et al. 2012, *ApJL*, 758, L41
- Thompson, T. A., Quataert, E., Zhang, D., & Weinberg, D. H. 2016, *MNRAS*, 455, 1830
- Tripp, T. M., Meiring, J. D., Prochaska, J. X., et al. 2011, *Science*, 334, 952
- Tumlinson, J., Thom, C., Werk, J. K., et al. 2013, *ApJ*, 777, 59
- Tumlinson, J., Peebles, M. S., & Werk, J. K. 2017, *ARA&A*, 55, 389
- Voit, G. M. 2005, *Reviews of Modern Physics*, 77, 207
- Weilbacher, P. M., Duc, P.-A., & Fritze-v. Alvensleben, U. 2003, *A&A*, 397, 545
- Werk, J. K., Prochaska, J. X., Thom, C., et al. 2012, *ApJS*, 198, 3
- Werk, J. K., Prochaska, J. X., Thom, C., et al. 2013, *ApJS*, 204, 17
- White, M., Blanton, M., Bolton, A., et al. 2011, *ApJ*, 728, 126
- White, M., Myers, A. D., Ross, N. P., et al. 2012, *MNRAS*, 424, 933
- Worseck, G., Prochaska, J. X., Hennawi, J. F., & McQuinn, M. 2016, *ApJ*, 825, 144
- Wright, E. L., Eisenhardt, P. R. M., Mainzer, A. K., et al. 2010, *AJ*, 140, 1868
- Yoon, J. H., & Putman, M. E. 2017, *ApJ*, 839, 117
- Young, L. M., Scott, N., Serra, P., et al. 2014, *MNRAS*, 444, 3408
- Zahedy, F. S., Chen, H.-W., Rauch, M., Wilson, M. L., & Zabludoff, A. 2016, *MNRAS*, 458, 2423
- Zhu, G., Ménard, B., Bizyaev, D., et al. 2014, *MNRAS*, 439, 3139